Water Science & Technology

Water Science & Technology Vol 89 No 8, 2006 doi: 10.2166/wst.2024.108

Identification, degradation characteristics, and application of a newly isolated pyridine-degrading *Paracidovorax* sp. BN6-4

Die Liang[a], Yifei Xie[b], Yi Jiang[a], Wenlai Xu[a], Zicheng Wang[c] and Dan Zhang[b,*]

[a] State Key Laboratory of Geohazard Prevention and Geoenvironment Protection, Chengdu University of Technology, Chengdu 610059, China
[b] CAS Key Laboratory of Environmental and Applied Microbiology, Environmental Microbiology Key Laboratory of Sichuan Province, Chengdu Institute of Biology, Chinese Academy of Sciences, Chengdu 610041, China
[c] School of Resource and Environmental Engineering, Mianyang Normal University, Mianyang 621000, China
*Corresponding author. E-mail: zhangdan@cib.ac.cn

ABSTRACT

The *Paracidovorax* sp. BN6-4 capable of degrading high concentrations of pyridine was isolated from the coking sludge. The removal rate of BN6-4 to 1,000 mg/L pyridine during 48 h was 97.49 ± 1.59%. The primary intermediate metabolites of pyridine degradation by strain BN6-4 were identified by gas chromatography-mass spectrometry (GC-MS), including N-Ethylurea, acetamidoacetaldehyde, and N-Hydroxymethylacetamide, etc. Subsequently, two different biodegradation pathways of pyridine were proposed. First, the hydroxylation of pyridine to form the intermediates pyridin-2(1H)-one and 5,6-dihydropyridine-2,5-diol, the former undergoing oxidative ring opening and the latter oxidative ring opening via N-C2 and C2–C3 ring opening to ammonia and carbon dioxide. Furthermore, the organic matter was greatly degraded by the bioremediation of real coking wastewater using BN6-4. This study enriched the microbial resource for pyridine degradation and provided new insights about the biodegradation pathway of pyridine, which is of great significance for the pyridine pollution control and coking wastewater treatment.

Key words: biodegradation, coking wastewater, metabolic, *Paracidovorax*, pyridine

HIGHLIGHTS

- *Paracidovorax* sp. BN6-4 was first isolated for pyridine degradation.
- BN6-4 achieved 97.49 ± 1.59% pyridine degradation at 1000 mg/L in 48 h at 30 °C and pH 7.0.
- Different pyridine metabolic pathways are first proposed in pyridine biodegradation.
- *Paracidovorax* sp. BN6-4 and carrier removed 1929 mg/L COD from coking wastewater.

GRAPHICAL ABSTRACT

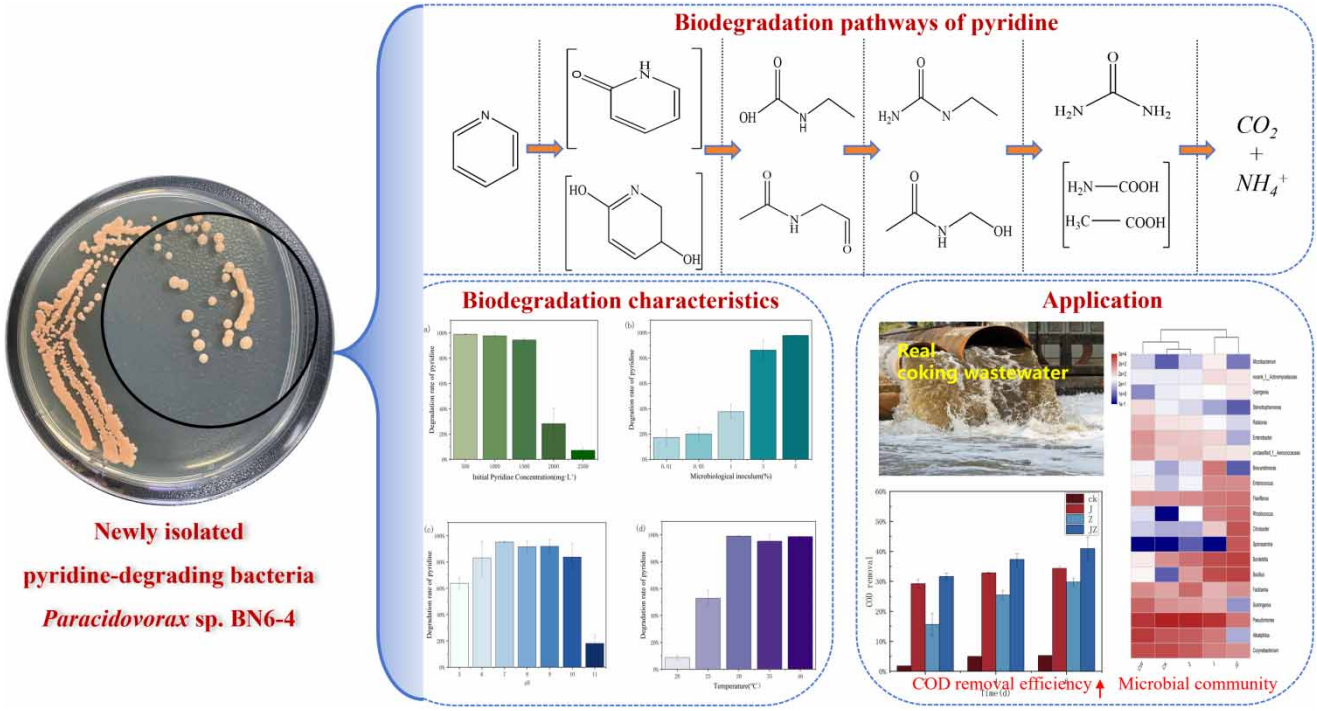

1. INTRODUCTION

Heterocyclic nitrogen compounds are organic compounds that contain a heterocyclic structure in their molecules. Among them, pyridine is a common six-membered heterocyclic compound widely used in the manufacture of pesticides, pharmaceuticals, and petroleum products (Qiao & Wang 2010). It is a volatile, odorous, and difficult to degrade organic pollutants (Meng *et al.* 2017). Due to their high solubility in water and high chemical stability, pyridine compounds are susceptible to entering groundwater systems by diffusion, leading to an increased risk of contamination of the aquatic environment (Watson & Cain 1975). Moreover, pyridine is moderately acutely toxic to living organisms and may cause biotoxicity, teratogenicity, and carcinogenicity. As a result, the U.S. Environmental Protection Agency has listed pyridine as one of the priority pollutants (Watson & Cain 1975; Shi *et al.* 2019). In addition to its ecosystem hazards, pyridine is strongly inhibitory to microorganisms and is difficult to degrade by natural oxidative decomposition, which increases the difficulty of self-purification of surface water and environmentally sound treatment of wastewater. Therefore, there is an urgent need to develop cost-effective pyridine treatment technologies to effectively remove or reduce the concentration of pyridine and lessen its negative impact on the environment and ecosystems to protect water resources and ecosystem health.

In addition, the mechanisms of microbial degradation of pyridine have only been extensively studied to a limited extent. Wang *et al.* (2018) isolated *Paracoccus* sp. NJUST30 during the degradation of pyridine, which produced intermediates such as 2,4-dihydroxy-2H-pyridine-3-one and 2-carboxylic acid, revealing a biodegradation pathway involving hydroxylation, pyridine ring cleavage, carbonylation, and carboxylation for pyridine. Shukla & Kaul (1974) found that *Corynebacterium* sp. generates formic acid, amines, and succinic semialdehyde during the degradation process. Deng's research found that *Achromobacter* sp. DN-06 degrades pyridine through a direct ring-opening mechanism, concurrently involving N-C2 and C2–C3 ring-opening pathways (Deng 2011). These studies indicate that the current understanding of the biodegradation mechanism of pyridine is limited, and different microbial species exhibit variations in pyridine degradation mechanisms. Some *Paracidovorax* sp. exhibit notable tolerance to organic solvents and have been predominantly employed for degrading organic compounds like polycyclic aromatic hydrocarbon (Singleton *et al.* 2009) and 4-nitrotoluene (Ju & Parales 2011). Nevertheless, research on the degradation of pyridine by acidophilic bacteria remains limited. Therefore, there is a compelling need for an in-depth investigation into the degradation traits of pyridine by acidophilic bacteria and the associated metabolic mechanisms.

In this study, a new efficient pyridine-degrading bacterium was isolated from the sludge at the coking plant's effluent, and it was molecularly identified as *Paracidovorax* sp. Although pyridine biodegradation investigations have been described, since *Paracidovorax* sp. is being used for pyridine degradation for the first time, a thorough investigation of their degradation properties and pathways is required. The purpose of this study was to investigate the effects of different initial pyridine concentrations, temperature, pH, and other environmental factors on the degradation of pyridine by the strains. Based on the intermediate products produced during pyridine biodegradation, a new degradation pathway for pyridine biodegradation by *Paracidovorax* sp. BN6-4 was proposed for the first time. In addition, pyridine-efficient degrading bacteria combined with carriers were applied to treat real coking wastewater. Strengthen the proliferation of indigenous microorganisms, increase microbial diversity, and change the structure of the microbial community. It can effectively degrade organic matter in wastewater and remove COD in wastewater. This study provides valuable supplementary information for the microbial pyridine degradation pathway and offers a new resource and theoretical basis for exploring efficient microbial pyridine remediation technology.

2. MATERIALS AND METHODS

2.1. Growth medium

The bacterial enrichment medium (EM) used for cultivating pyridine-degrading bacteria is a minimal salt media (MSM) containing pyridine and composed of the following components: MgSO4·7H_2O 0.2 g, Na_2HPO_4 4.26 g, KH_2PO_4 2.65 g, $CaCl_2$ 0.02 g, 1 mL trace elements, distilled water 1,000 mL, pH = 7, pyridine concentration adjusted as per experimental requirements. Sterilized at 121 °C for 20 min. Trace elements stock solution: KI 0.005 g, $MnSO_4$·4H_2O 0.2 g, $CuSO_4$·5H_2O 0.02 g, $ZnSO_4$·7H_2O 0.2 g, Na_2MoO_4·2H_2O 0.25 g, H_3BO_3 0.008 g, $FeCl_3$ 0.1 g, diluted to 100 mL with water.

Luria Bertani (LB) medium is employed to amplify bacterial cultures for the investigation of their degradation characteristics and metabolic pathways. It comprises peptone 10 g, yeast extract 5 g, NaCl 10 g, diluted to 1L with deionized water, pH = 7.4–7.6, sterilized at 121 °C for 20 min. The solid medium, used for strain preservation, was prepared by incorporating agar into the LB medium.

2.2. Isolation of pyridine-degrading bacteria

Pyridine-degrading strains were isolated from the sludge at the Chongqing Coking Plant. To enrich pyridine-degrading bacteria, 90 mL of MSM and 2 g of sludge were introduced into 150 mL conical flasks, with pyridine as the sole carbon and nitrogen source. The initial pyridine concentration was 30 mg/L, and every 7 days, 10 mL of the enrichment solution was transferred to a new enrichment medium. The concentration of pyridine in the medium was gradually increased to 300 mg/L (30, 90, 180, 240, 300 mg/L). To isolate pyridine-degrading bacteria, 1 mL of the enrichment medium suspensions was aseptically transferred to a sterile test tube and diluted with sterile water ($10^{-1} \sim 10^{-8}$). Subsequently, the diluted bacterial suspension was evenly spread onto solid LB plates containing inactivated bacteria. These plates were placed in a constant-temperature incubator at 30 °C for 48 h. Well-developed colonies with distinctive morphologies were selected for further purification through 3–4 rounds of streaking. These purified isolates were then transferred and maintained on a solid LB slant medium. The isolated strains were subsequently inoculated into MSM containing pyridine and incubated at 30 °C with a pH of 7 and a rotational speed of 150 rpm. The concentration of pyridine in the medium was determined after 48 h of incubation. Among these strains, the one exhibiting the highest pyridine degradation rate was labeled as BN6-4.

2.3. Identification of strain BN6-4

The strain BN6-4 was subjected to Gram staining to observe its cellular morphology under an optical microscope. For the identification of the obtained pyridine-degrading strain, a 16S rRNA gene sequence analysis was performed. A culture of the strain in an LB liquid medium for 1 day was used for DNA extraction. A 300 μL aliquot of bacterial culture was processed using the Ezup column soil DNA extraction kit to extract the strain's DNA. The bacterial DNA was then subjected to PCR amplification using the universal bacterial primers 27F (5′-AGAGTTTGATCATGGCTCAG-3′) and 1492R (5′-GGTTACCTTGTTACTACTT-3′). Following gel electrophoresis confirmation of PCR products, they were sent to Sangon Biotech for sequencing. Sequencing results were uploaded to the NCBI database for gene alignment, providing a preliminary determination of the strain's species. Furthermore, a phylogenetic tree was constructed using MEGA 7.0. Metabolic characteristics of the microorganism were assessed through biochemical experiments, including sugar metabolism, enzyme activity, and redox reactions.

2.4. Biodegradation characteristics of strain BN6-4

The pyridine degradation experiment using strain BN6-4 was carried out in 500 mL conical flasks, each containing MSM with pyridine. Initially, the pyridine-degrading bacterium BN6-4 was cultured in an LB liquid medium at 30 °C with a rotational speed of 150 rpm for 48 h. After incubation, the culture solution was centrifuged at 10,000 rpm for 5 min, and the supernatant was discarded. The bacterial cells were then washed two to three times with a sterilized inorganic salt medium. Following these washes, the bacterial cells were resuspended in MSM to reach an optical density (OD600) of 1 at a wavelength of 600 nm, resulting in the preparation of the seed solution. Subsequently, this seed solution was used for the pyridine degradation experiments in the conical flasks containing MSM. The degradation characteristics of BN6-4 on pyridine were investigated through single-factor experiments. In the experiment to assess the impact of initial concentrations, a 5% BN6-4 seed solution was inoculated into MSM containing varying initial pyridine concentrations (500, 1,000, 1,500, 2,000, 2,500 mg/L). The incubation was conducted at 30 °C, with a pH of 7 and agitation at 150 rpm for 48 h. Samples were collected to measure the pyridine concentration, and the degradation rate was subsequently calculated. In the temperature experiments, the incubation temperature was set at 20, 25, 30, 35, and 40 °C. The pH was maintained at 7, and the rotational speed was set at 150 rpm. For the experiment investigating the effect of inoculum amount on microbial pyridine degradation, the inoculum amounts were set at 0.1, 0.5, 1, 3, and 5%, respectively. The BN6-4 seed culture was inoculated into MSM containing 1,000 mg/L pyridine at a 5% inoculation rate, with shaking at 150 rpm and incubation at 30 °C. In the pH experiment, the initial pH was adjusted to 5.0, 6.0, 7.0, 8.0, 9.0, 10.0, and 11.0 using 1 mol/L HCl and 1 mol/L NaOH. Samples were taken after 48 h of incubation to measure pyridine concentration and calculate the degradation rate.

2.5. Metabolic pathway analysis of pyridine

Samples during pyridine degradation by the strain were filtered through a 0.45 μm filter membrane, and 30 mL of filtrate was extracted three times with an equal volume of ethyl acetate under neutral and acidic conditions, respectively. The extraction solution was filtered through anhydrous sodium sulfate and then concentrated to 1 mL using a rotary evaporator. Specific intermediates in the metabolism were determined by GCMS-QP-2010. Samples were first taken at different times of pyridine degradation, filtered through a 0.45 μm membrane, and then extracted three times with equal volumes of ethyl acetate in 30 mL of filtrate under neutral and acidic conditions, respectively. The extracts were filtered through anhydrous sodium sulfate baked at 400 °C for 7 h and then concentrated to 1 mL using a rotary evaporator. The extracts were analyzed by GC-MS under the following operating conditions: inlet and detector temperatures of 250 °C, flow rate of 1 mL/L, heating program of 0 °C/min to 250 °C, holding time of 3 min, and a carrier gas of He. The conditions for mass spectrometry (MS) analysis included an ionization voltage of 70 eV, a full-ion scan at 50–625 m/z, an ion source of 250 °C, and an electronic capability of 70 eV. Peak detection and mass spectral peak integration were performed on the detected sample mass spectral data. The molecular formulas and structures of compounds are determined by comparing the mass spectra with those of known compounds in the NIST20 spectral library.

2.6. The application of BN6-4 on real coking wastewater

The ability of strains and carriers combined to treat coking wastewater was evaluated in shake flask experiments. PBS granules and activated carbon powder were heated at 185 °C and combined with stirring to make the carriers. The biodegradation of coking wastewater was organized into four groups: CK, which served as the control and received 100 mL of coking wastewater; J, which involved the addition of 5% (w/v) strain BN6-4; Z, which involved the addition of 5% (w/v) carriers; and JZ, which involved the addition of 5% (w/v) of carriers and strain BN6-4. The running time was 6 days, and the conditions of the operation were 30 °C and 150 rpm. Samples were taken every 2 days to analyze the COD removal rate. The samples were centrifuged and the supernatant was discarded for NextSeq Illumina.

2.7. Analytical methods

The pyridine concentration was determined using UV spectrophotometry. This involved scanning the UV spectrum of pure pyridine to identify its maximum absorption wavelength, which was found to be 256 nm. Five pyridine concentration gradients (0, 10, 50, 100, and 150 mg/L) were prepared, and their absorbance was measured to construct the pyridine standard curve. The bacterial suspension was introduced into the pyridine inorganic salt medium, and samples were collected to measure the absorbance after a specified incubation period. The concentration was then determined by fitting the absorbance value to the standard curve (Li & Zhao 2001). The pyridine and COD degradation rates were calculated by the formula

((C0 – C1)/C0) × 100%, where C0 is the concentration of pyridine after degradation in the control group (mg/L), and C1 is the concentration of pyridine after degradation in the experimental group (mg/L). In this study, three separate typical organic matter degradation tests were conducted. The results for COD, biomass (OD600), and pyridine concentration are expressed as mean ± SD (standard deviation).

3. RESULTS AND DISCUSSION

3.1. Isolation and identification of pyridine-degrading bacteria

After five rounds of consecutive enrichment, a highly efficient pyridine-degrading bacterium, BN6-4, was isolated from sludge samples collected from a coking plant. Following 24 h of cultivation on LB solid medium, BN6-4 exhibited morphological characteristics on LB agar plates, as depicted in S1. In the image, BN6-4 formed large, circular colonies with well-defined edges, displaying an orange-pink color and a smooth surface. The morphological characteristics of BN6-4 under an optical microscope are shown in S1B, where it appeared rod-shaped and tested Gram-positive.

Partial physiological and biochemical test results for strain BN6-4 are presented in S3. Among the three carbon sources tested, strain BN6-4 demonstrated the ability to utilize glucose and sucrose but not lactose. Additionally, strain BN6-4 exhibited positive reactions in oxidation enzyme tests, starch hydrolysis tests, lipase tests, urease tests, methyl red tests, V-P tests, and Gram staining reactions. The 16S rDNA of strain BN6-4 was amplified through PCR, and sequencing resulted in an 855bp-long sequence. This obtained sequence was then compared to sequences already registered in the GenBank database using BLAST. A phylogenetic tree was constructed using MEGA-X software (as shown in S4), which provided initial identification of BN6-4 as belonging to the *Paracidovorax* sp.

3.2. Characteristics of pyridine degradation by BN6-4

To evaluate BN6-4's pyridine degradation capacity, the bacteria were introduced into a pyridine MSM at a concentration of 1,072.74 mg/L. The conditions included a pH of 7.0, a temperature of 30 °C, and agitation at 150 rpm, with a 5% inoculum size. Figure 1 illustrates BN6-4's growth curve and pyridine degradation in the pyridine MSM. There exists a positive correlation between pyridine degradation and bacterial growth. During the initial 0–24 h, BN6-4 exhibited a slow growth rate. Between 24 and 48 h, the bacterial culture entered the logarithmic growth phase, indicating that the strain required an extended adaptation period in the pyridine-containing MSM before achieving exponential growth. Remarkably, by the 48-h mark, the pyridine degradation rate had reached an astonishing 99.23 ± 0.24%. While the pyridine concentration in the medium declined gradually from 0 to 24 h, it experienced a rapid reduction from 24 to 48 h. At the 48-h point, the pyridine degradation rate had reached an impressive 99.23 ± 0.24%. After 48 h, bacterial growth stabilized, and the residual pyridine concentration began to level off.

It is important to highlight that pyridine possesses certain toxic properties, including teratogenic and mutagenic effects (Watson & Cain 1975). Consequently, elevated pyridine concentrations can impede microbial growth and result in

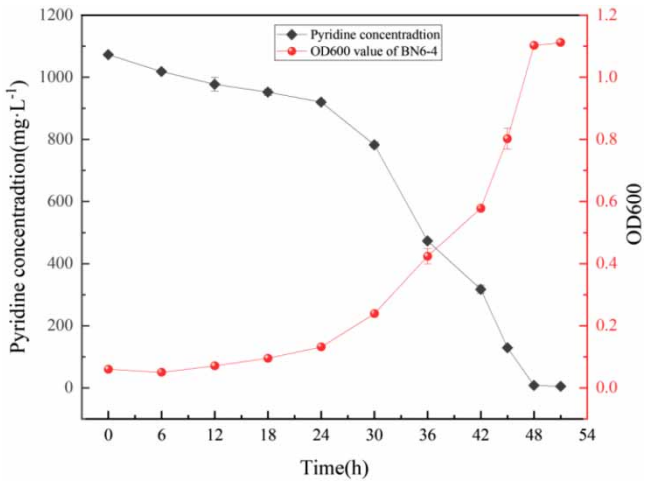

Figure 1 | The growth curves of BN6-4.

diminished degradation efficiency. As depicted in Figure 2(a), BN6-4 exhibited consistent pyridine degradation rates exceeding 90% even at initial pyridine concentrations ranging from 500 to 1,500 mg/L. This resilience suggests the strain's robust tolerance and resistance to pyridine. The highest degradation rate, reaching 97.68 ± 2.16%, was observed at an initial pyridine concentration of 1,000 mg/L. However, upon further elevating the pyridine concentration to 2,000 mg/L, the strain's degradation rate plummeted to 28.17%, signifying a notable drop in efficiency. At 2,000 mg/L, degradation efficiency sharply decreased to 7.12 ± 2.07%, underscoring the inhibitory effect of high pyridine concentrations on microorganisms, potentially by suppressing their growth and metabolic activities. This could be attributed to the toxic impact of pyridine at elevated concentrations on microbial cell membranes or metabolic pathways.

The amount of microbial inoculum impacts the density and activity of the microbial population, which influences the pace and efficiency of pyridine breakdown. Figure 2(b) shows the effect of inoculum size on pyridine degradation by BN6-4. With an increase in the quantity of microbial inoculum, the efficiency of pyridine breakdown improved. The highest degradation efficiency of 97.94 ± 0.23% was observed for pyridine at 5% inoculum concentration. This is because higher inoculum concentration helps to initiate the degradation process faster at the initial stage. In addition, high inoculum populations of microorganisms may be more resistant to the toxicity of organic matter, whereas high inoculum levels may minimize the detrimental effects of toxicity on microorganisms. Consequently, the higher the microbial population, the more likely it is that the organic matter will be completely degraded and the more likely it is that the concentration of residues will be reduced. Higher the microbial population, the more likely it is that the organic matter will be completely degraded and the concentration of residues reduced.

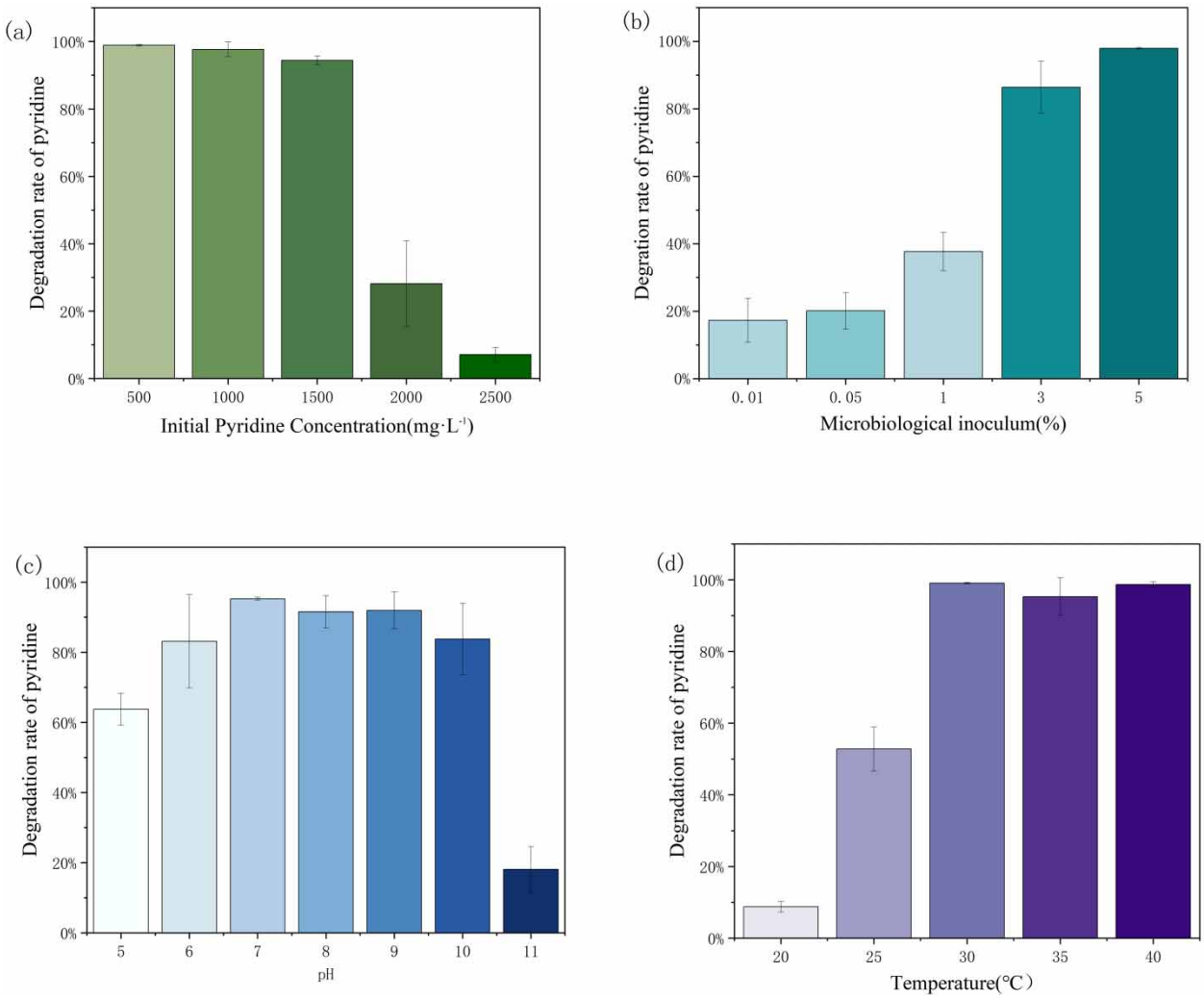

Figure 2 | Effects of different environmental factors on the degradation of pyridine by BN6-4.

The pyridine molecule undergoes ionization at different pH conditions, thus changing its solubility and reactivity. Under acidic conditions, pyridine may exist in a molecular form, while under alkaline conditions it may exist in an ionic form. This ionized state may impact pyridine's bioaccessibility when degraded by microbes. In addition, microorganisms exhibit the highest activity in a specific pH range. Different microbial strains may have different optimal pH ranges, and the pH of the medium plays a crucial role in microbial growth, metabolism, enzyme activity, and ecological interactions, so choosing the right pH range optimizes the efficiency of microbial degradation of pyridine and ensures that the microorganisms can maximize their degradation potential in the most suitable environment. Figure 2(c) shows the effect of pH on the degradation of pyridine by BN6-4. The bacterium was able to degrade pyridine with more than 80% efficiency in the pH range of 6–10. It is noteworthy that BN6-4 showed superior degradation performance under alkaline (7–10) conditions as compared to acidic conditions (5–7). The optimum pH value for pyridine degradation by BN6-4 was pH 7 with a maximum degradation efficiency of 95.27 $\pm$ 0.42%. This indicates that the enzyme activity of BN6-4 is the most suitable for the growth of the bacterium under neutral conditions. The degradation rate of pyridine was 83.79% at pH 10, but the degradation rate decreased sharply to 18.08 $\pm$ 6.5% when the pH was increased to 11. This indicates that pH is very critical for microbial degradation of pyridine.

Temperature is a key environmental factor affecting microbial growth and substrate degradation because important components of microbial cells (e.g., proteins and nucleic acids) are temperature sensitive. Different microorganisms and enzymes have different optimum temperatures. Figure 2(d) shows the effect of temperature on pyridine degradation by BN6-4. At 20 °C, the degradation rate of pyridine was only 8.79% $\pm$ 1.51%, which indicated that pyridine degradation was significantly inhibited at low temperatures, suppressing the growth and metabolic rate of the microorganisms. The highest removal rate of pyridine was achieved at 30 °C with 99.05 $\pm$ 0.22%. This indicates that 30 °C is the optimum temperature for microbial growth and the microbial degradation activity is the highest. It is noteworthy that a decrease in degradation rate was observed at 35 °C, but there was an increase in degradation rate at 40 °C. This may be because pyridine is less toxic and more easily degraded at a high temperature of 40 °C.

3.3. Pyridine degradation pathway of BN6-4

3.3.1. Intermediate metabolites of pyridine degradation by BN6-4

Given the structural similarity of pyridine to benzene rings, pyridine possesses inherent aromaticity. Hence, initial investigations employed UV scanning to determine if BN6-4 produces cyclic structural intermediates during pyridine degradation. Pyridine exhibits two distinct UV absorption bands: one at 240 ~ 260 nm ($\varepsilon = 2000$), corresponding to π–π^* transitions (akin to benzene), and another at 270 nm, corresponding to $n \rightarrow \pi^*$ transitions ($\varepsilon = 450$). Analysis of the UV scanning data (Figure 3) revealed that during the process of pyridine degradation by strain BN6-4, the peak in the UV absorption

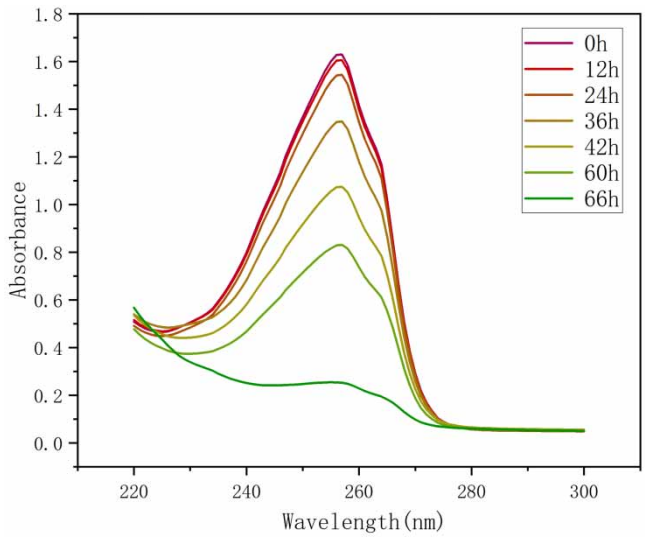

Figure 3 | UV scan of the BN6-4 pyridine degradation process product.

spectrum of pyridine remained relatively unchanged, with only a slight redshift occurring at 36 h. This suggests the presence of a small quantity of hydroxyl groups during BN6-4-mediated pyridine degradation, which are quickly utilized and degraded by BN6-4 (Figure 4).

GC-MS analysis was employed to identify the major metabolites formed during pyridine degradation by strain BN6-4 (Figure 4). Table 1 summarizes the main intermediate metabolites detected during the biodegradation of pyridine, along with their molecular formulas, structures, retention times, and molecular weights. Among these, B1, with an m/z of 79 and a chemical formula of C_5H_5N, was identified as pyridine, with a retention time of 7.15 min. B2, identified as N-Ethylurea with an m/z of 88 and a molecular formula of $C_3H_8N_2O$, may be the result of an amino group substituting the oxygen in pyridine during oxidative ring opening. B3, urea, with an *m/z* of 60, is generated by the carbon–nitrogen bond cleavage of N-Ethylurea. Metabolite B4, acetamidoacetaldehyde, with an *m/z* of 101 and a molecular formula of $C_4H_7O_2$, is formed when pyridine undergoes N-C2 and C2–C3 ring opening simultaneously. B5, N-Hydroxymethylacetamide, with an *m/z* of 89 and a molecular formula of $C_3H_7NO_2$, is reduced from acetaldehyde acetamidoacetaldehyde.

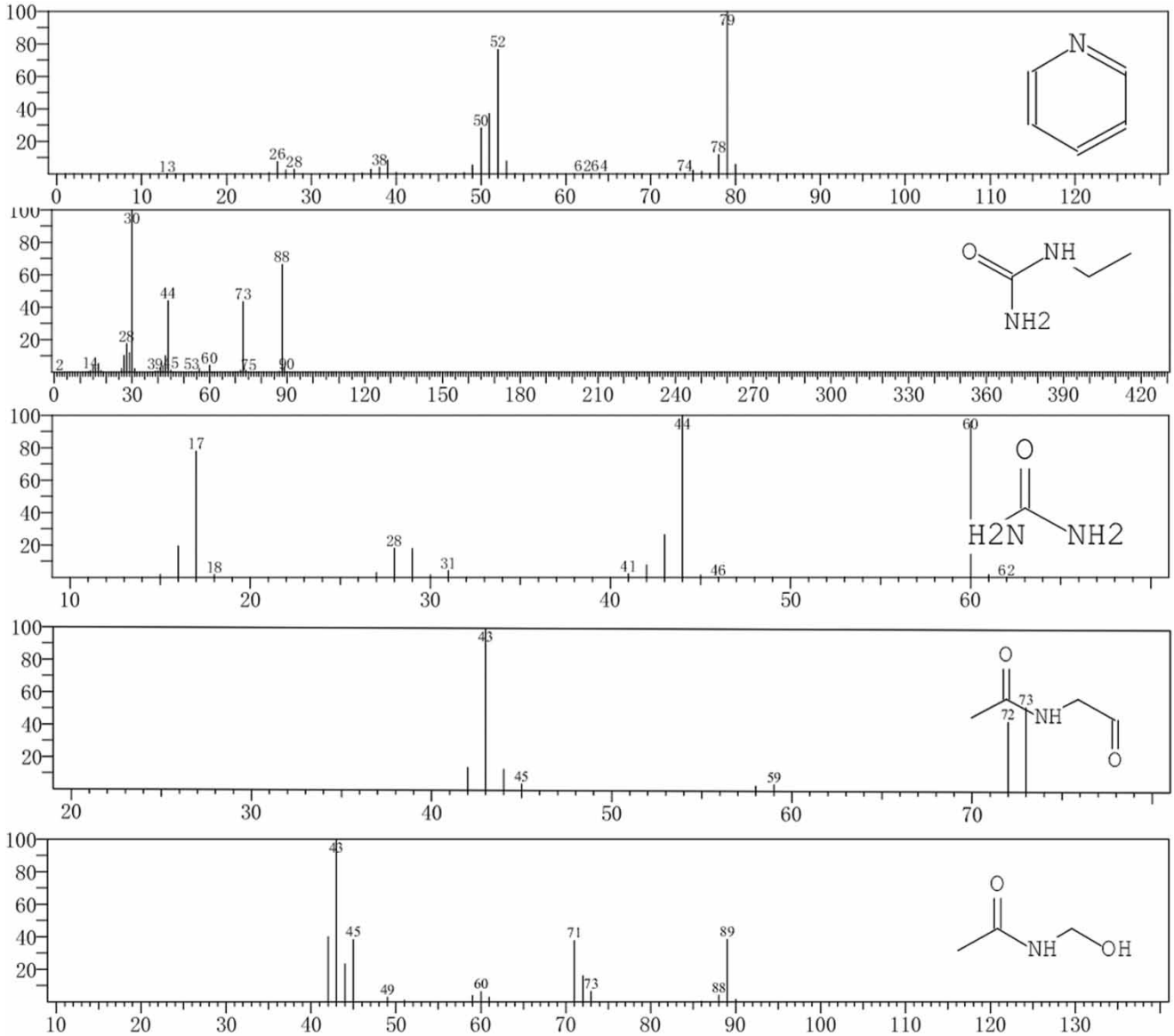

Figure 4 | Mass spectrometric analysis of metabolites (B1–B5) during the biodegradation of Pyridine in BN6-4.

Table 1 | Intermediate metabolites were identified during pyridine degradation by BN6-4 through GC-MS analysis

Metabolite	Compound	Formula	Calculated mass	Mass-to-charge Ratio (*m/z*)
B1	Pyridine	C5H5N	79.10	79
B2	N-Ethylurea	C3H8N2O	88.11	88
B3	Urea	CON2H2	60.06	60
B4	Acetamidoacetaldehyde	C4H7NO2	101.10	101
B5	N-Hydroxymethylacetamide	C3H7NO2	89.09	89

3.3.2. Inference of the pyridine biodegradation pathway by BN6-4

There are two main degradation pathways for pyridine, one is direct reductive cleavage without hydroxylation; the other is hydroxylation of the pyridine ring and then ring opening, including methylation (Nie *et al.* 2021), hydroxylation (Casaite *et al.* 2020), carboxylation (Zhang *et al.* 2014), and carbonylation (Singh & Lo 2017) pathways. Previous studies have proposed hydroxylation of the pyridine ring as the initial step in the pyridine degradation pathway, leading to the formation of various intermediate products (Wang *et al.* 2018). Watson and collaborators isolated *Bacillus* and *Nocardia* strains from the soil. Under the presence of 0.20 mM KCN, *Bacillus* accumulated formate and potential formamide from pyridine. Using [14C]-labeled pyridine, it was revealed that the pyridine degradation by *Bacillus* occurs through the cleavage of the pyridine ring between C2 and C3. Nocardia's pyridine degradation process produced succinic semialdehyde, indicating that the cleavage of the pyridine ring took place between N and C2 (Watson & Cain 1975). As shown in Figure 5, based on the analysis of pyridine intermediate metabolites by strain BN6-4, we propose two potential pyridine biodegradation pathways. Pathway I begins with the hydroxylation of pyridine, leading to the formation of pyridine-2(1H)-one, followed by oxidative ring opening to generate the intermediate N-Ethylurea, which subsequently undergoes carbon–nitrogen bond cleavage to produce urea. Finally, urea is converted into ammonia and CO_2. Pathway II commences with pyridine hydroxylation, resulting in the formation of 5,6-dihydropyridine-2,5-diol as an intermediate. This intermediate undergoes N-C2 and C2–C3 ring opening to yield metabolite acetamidoacetaldehyde, which is subsequently reduced to N-Hydroxymethylacetamide, eventually transforming into ammonia and CO_2. This analysis suggests that the efficient pyridine-degrading bacterium BN6-4 employs two distinct biodegradation pathways, distinct from previously reported pyridine degradation systems, thereby expanding the understanding of pyridine biodegradation.

3.4. Application of BN6-4 in real coking wastewater

Coking wastewater is produced during the refining operations of many industrial products, including coal coking, coal gas purification, as well as the processing of copper and steel. Its chemical composition is notably influenced by the coal's constitution and the characteristics of the manufacturing procedures. Typically, coking wastewater contains high concentrations

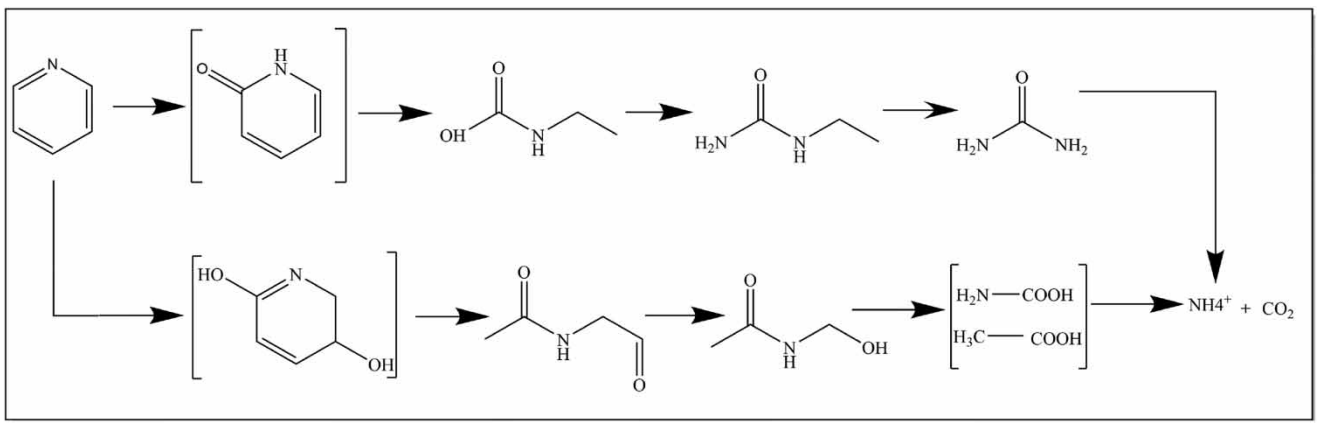

Figure 5 | Proposed pyridine biodegradation pathways by the strain BN6-4.

of both inorganic and organic pollutants, such as ammonia, sulfides, phenolic resins, polycyclic aromatic hydrocarbons (PAHs), and nitrogen-containing heterocyclic compounds. Pyridine, indole, and quinoline are common examples of nitrogen-containing organic pollutants in this context (Ma *et al.* 2015; Zhao & Liu 2016). Microbial immobilization techniques find extensive application in the treatment of complex pollutants. For example, Niu *et al.* (2023) work involved immobilizing the J2 strain with biochar, achieving a degradation rate of 98.66 ± 0.47% for wastewater containing 2,000 mg/L of pyridine. Additionally, research by Cao suggests that employing immobilized mixed microbial communities for degrading PAH in wastewater can effectively harness the role of microorganisms in treating recalcitrant wastewater and improve water quality (Cao 2022).

In the experiment of microbial degradation of coking wastewater containing 4,711.20 mg/L COD, the addition of strain BN6-4 and carrier had a certain effect on COD removal. The results are shown in Figure 6, where COD removal increased with time on days 2, 4, and 6 of the experiment. For the coking wastewater with an initial COD concentration of 4,711.20 mg/L, the removal rates of group J were 29, 32, and 35% on days 2, 4, and 6, respectively. This indicates that *Paracidovorax* sp. BN6-4 has adapted to coking wastewater containing pyridine, PAHs, and other organic pollutants and can effectively degrade specific pollutants in the wastewater. Compared to the CK group, the COD removal in Z was less than 15.62% in 2 days and increased to 29.78% in 6 days. This indicates that the carriers provide nutrients and shelter space for indigenous microorganisms, thus accelerating the rate of biodegradation in wastewater. Most importantly, the COD removal was higher in the JZ group at 2, 4, and 6 days as compared to the CK, J, and Z groups. It was 31.61, 37.30, and 40.95%, respectively. It reduced COD from 4,711.20 to 2,781.88 mg/L in just 6 days. These results suggest that the combination of strain BN6-4 and carrier can effectively enhance the microbial treatment of real coking wastewater.

3.4.1. Ultraviolet scanning during degradation of coking wastewater

Previous studies have shown that, in addition to glucose, organic matter in water also has significant absorption in the UV spectral range of 240–300 nm. The results of full-wavelength UV scanning of coking wastewater treated for 6 days are shown in Figure 7, and group CK exhibited significant absorption peaks in the wavelength range of 260–280 nm. In contrast, groups J, Z, and JZ showed no absorption peaks. This observation indicates that the organic matter in the coking wastewater was effectively degraded. It is noteworthy that the JZ group showed significantly lower UV absorption in the spectra compared to the other groups, suggesting that the combination of *Paracidovorax* sp. BN6-4 with the carrier was more effective in the treatment of coking wastewater. This study highlights the potential of the combination of carriers and acid-eating bacteria for the treatment of actual coking wastewater, providing valuable theoretical and practical insights into the microbial remediation of coking wastewater.

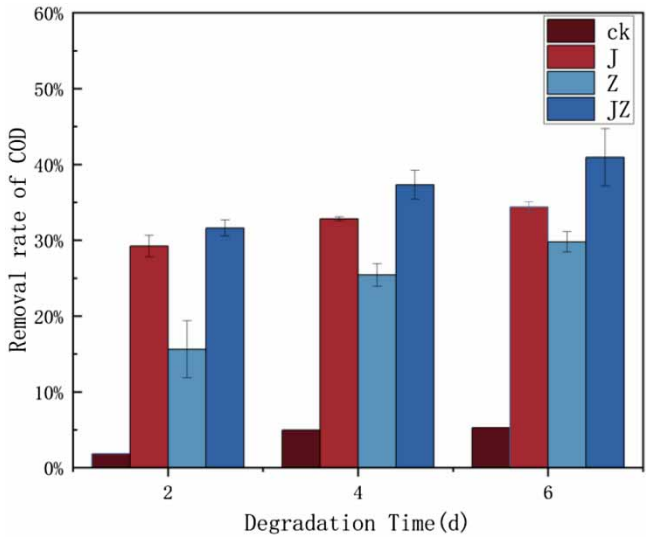

Figure 6 | Removal rate of COD from coking wastewater (CK, blank control, add 100 mL of coking wastewater; J, add 5% strain BN6-4; Z, add of 5% carriers; JZ, add 5% carriers and strain BN6-4).

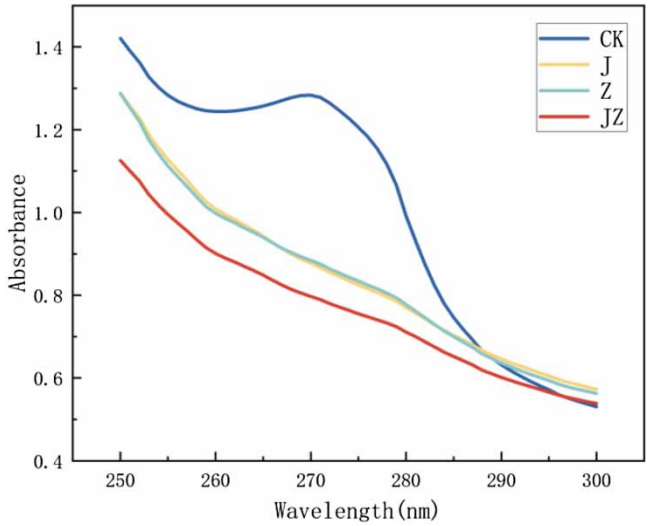

Figure 7 | 6d UV scanning of degraded substances in coking wastewater.

3.4.2. Microbial community composition and structure

To understand the changes in microbial community structure during the treatment of coking wastewater, the treatment effects exhibited by different systems were analyzed. The Alpha diversity index in Table 2 reveals that the JZ group, which included both strains and carriers, had a higher Shannon diversity index than the other groups and a lower Simpson index. It indicates that the BN6-4 strain and carriers greatly increase the abundance and diversity of the microbial community. To further evaluate the impact of these additions on microbial community structure, we performed a heatmap for the top 20 detected strains (Figure 8). The microbial species and abundances in group J and group JZ were changed, with group JZ showing a significant increase in the relative abundance of *Bacillus*, *Rhodococcus*, *Enterococcus*, and *Bordetella* compared to the control groups CK and CW. This suggests that adding strains promotes the growth of native microorganisms and boosts the prevalence of dominant bacteria. Conversely, the relative abundances of *Soehngenia* and *Alkaliphilus* decreased, indicating increased interspecies competition throughout treatment and a decline in dominance with the addition of the potent degrading strain BN6-4. In the JZ group, *Citrobacter*, *Sporosarcina*, *Bacillus*, *Rhodococcus*, and *Enterococcus* emerged as dominant bacteria, with significantly higher relative abundances than those in other groups. *Rhodococcus* is effective in degrading phenolic compounds and nitrogenous organic pollutants such as pyridine (Bai *et al.* 2022), *Sporosarcina Sporosarcina* destroyed polycyclic aromatic hydrocarbons (PAHs), and *Bacillus* degraded 100 phenol and 40 mg/L cyanide in coking wastewater (Rai *et al.* 2021). Enterococcus is effective in decomposing organic compounds such as pyridine (Nie *et al.* 2021), phenolic compounds (Huang *et al.* 2016), and PAHs (Li *et al.* 2018). The results of the UV scanning further demonstrated that the organic compounds in the coking wastewater were broken down. This suggests that the strains of bacteria that are capable of breaking down organic compounds, such as phenolic compounds and nitrogen-containing heterocyclic compounds, multiplied greatly in the coking wastewater and broke down the organic compounds into other small molecules. Thus, it can be inferred that the addition of strains and carriers will stimulate the growth of indigenous organic matter-degrading bacteria (*Enterobacter*,

Table 2 | Alpha diversity of coking wastewater samples before and after degradation

Sample	Shannon	Simpson	Ace	Chao	Coverage
CW	1.722228	0.236114	33.842905	33.25	0.999961
CK	1.319779	0.390641	31.849621	29.5	0.999922
J	1.985617	0.202563	34.01725	32.6	0.999941
Z	1.562773	0.338966	35.335875	32	0.999922
JZ	2.077207	0.153448	29.140537	28	0.999922

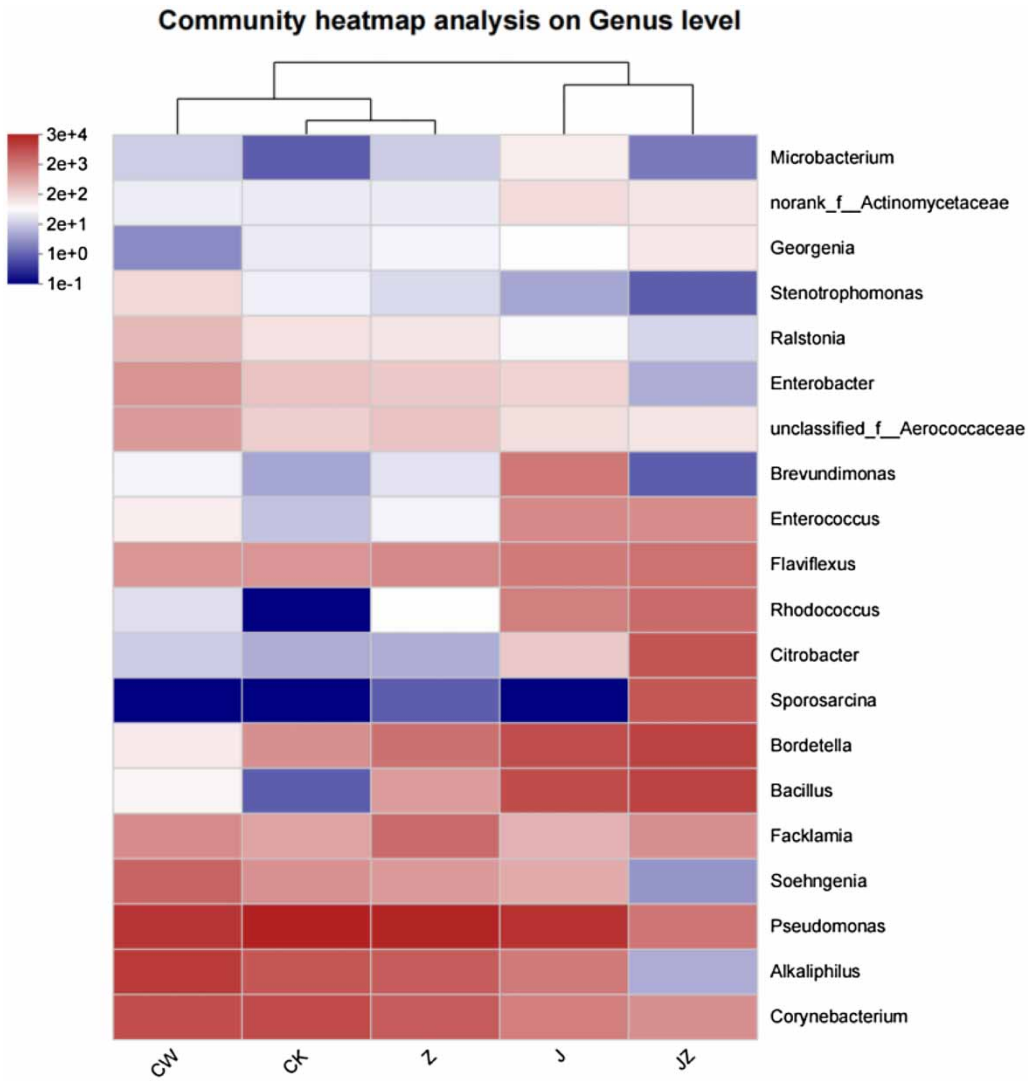

Figure 8 | Heatmap profiles showing the top 20 genera in the coking wastewater (CW denotes coking wastewater before degradation).

Bacillus, *Sporosarcina*, and *Rhodococcus*), increase the microbial diversity, and alter the microbial community structure of coking wastewater.

4. CONCLUSION

In this study, a novel pyridine-degrading strain BN6-4 was successfully isolated from coking sludge. The BN6-4 was identified by 16S rDNA as *Paracidovorax* sp. This strain was capable of growing solely on pyridine. Furthermore, *Paracidovorax* sp. BN6-4 demonstrated significant pyridine resistance and rapid breakdown rates. Within 48 h, BN6-4 achieved a degradation rate of 97.49 $\pm$ 1.59% for pyridine at an initial concentration of 1,500 mg/L. Furthermore, BN6-4 demonstrated growth capabilities across a temperature range of 20–40 °C, with optimal degradation efficiencies consistently above 90%. Between 30 and 40 °C, BN6-4 was found to thrive within a pH range of 5-10, with a maximal degradation rate of 95.27 $\pm$ 0.42% at pH 7. Additionally, increasing the inoculum size led to faster deterioration, with a rate of 97.94 $\pm$ 0.23% at 5% inoculum size. Through GC-MS analysis, a novel pyridine degradation pathway for strain BN6-4 was proposed, involving pyridine hydroxylation, N-C2, and C2–C3 ring-opening reactions. After the BN6-4 was applied to real coking wastewater, the results showed that the combination of *Paracidovorax* sp. BN6-4 and the carrier increased the removal rate of COD in real coking

wastewater, changed the structure of the microbial community, stimulated the growth of indigenous microorganisms, and improved the degradation ability of the microbial community on pollutants.

ACKNOWLEDGEMENTS

This work was supported by the Strategic Biological Resources Capacity Building Project of the Chinese Academy of Sciences [grant number KFJ-BRP-009-004] and the Key Research and Development Program of Sichuan Province [grant number 2020YFS0021].

DATA AVAILABILITY STATEMENT

All relevant data are included in the paper or its Supplementary Information.

CONFLICT OF INTEREST

The authors declare there is no conflict.

REFERENCES

Bai, X., Nie, M., Diwu, Z., Wang, L., Nie, H., Wang, Y., Yin, Q. & Zhang, B. 2022 Simultaneous biodegradation of phenolics and petroleum hydrocarbons from semi-coking wastewater: Construction of bacterial consortium and their metabolic division of labor. *Bioresource Technology* **347**, 126377.

Cao, K. 2022 Research on the application of microbial immobilization technology in the treatment of wastewater containing heavy metals. *World Nonferrous Metals* **5**, 214–216.

Casaite, V., Stanislauskiene, R., Vaitekunas, J., Tauraite, D., Rutkiene, R., Gasparaviciute, R. & Meskys, R. 2020 Microbial degradation of pyridine: A complete pathway in *Arthrobacter* sp. strain 68b deciphered. *Applied and Environmental Microbiology* **86** (15), 902–920 .

Deng, X. 2011 *Isolation, Degradation Characteristics and Metabolic Pathways of Functional Bacteria for the Degradation of Nitrogen Heterocyclic Compounds in Coking Wastewater*. Doctorate, South China University of Technology, Guangzhou, Guangdong, China.

Huang, Y., Hou, X., Liu, S. & Ni, J. 2016 Correspondence analysis of bio-refractory compounds degradation and microbiological community distribution in anaerobic filter for coking wastewater treatment. *Chemical Engineering Journal* **304**, 864–872.

Ju, K. S. & Parales, R. E. 2011 Evolution of a new bacterial pathway for 4-nitrotoluene degradation. *Molecular Microbiology* **82** (2), 355–364.

Li, Y. & Zhao, C. 2001 Determination of major pollutants in coking wastewater by ultraviolet spectrophotometry. *China Water Supply and Drainage* **17** (01), 54–56.

Li, J., Luo, C., Zhang, D., Song, M., Cai, X., Jiang, L. & Zhang, G. 2018 Autochthonous bioaugmentation-modified bacterial diversity of phenanthrene degraders in PAH-contaminated wastewater as revealed by DNA-stable isotope probing. *Environmental Science & Technology* **52** (5), 2934–2944.

Meng, Z., Chengda, H. & Weihui, L. 2017 Purification of refractory pyridine waste gas by anoxic denitrification. *Chinese Journal of Environmental Engineering* **11**(12), 6345–6350.

Ma, Q., Qu, Y., Shen, W., Zhang, Z., Wang, J., Liu, Z., Li, D., Li, H. & Zhou, J. 2015 Bacterial community compositions of coking wastewater treatment plants in steel industry revealed by Illumina high-throughput sequencing. *Bioresource Technology* **179**, 436–443.

Nie, Z., Yan, B., Xu, Y., Awasthi, M. K. & Yang, H. 2021 Characterization of pyridine biodegradation by two *Enterobacter* sp. strains immobilized on *Solidago canadensis* L. stem derived biochar. *Journal of Hazardous Materials* **414**, 125577.

Niu, H., Nie, Z., Long, Y., Guo, J., Tan, J., Bi, J. & Yang, H. 2023 Efficient pyridine biodegradation by *Stenotrophomonas maltophilia* J2: Degradation performance, mechanism, and immobilized application for wastewater. *Journal of Hazardous Materials* **459**, 132220.

Qiao, L. & Wang, J. L. 2010 Microbial degradation of pyridine by *Paracoccussp* isolated from contaminated soil. *Journal of Hazardous Materials* **176** (1–3), 220–225.

Rai, A., Gowrishetty, K. K., Singh, S., Chakrabarty, J., Bhattacharya, P. & Dutta, S. 2021 Simultaneous bioremediation of cyanide, phenol, and ammoniacal-N from synthetic coke-Oven wastewater using *Bacillus* sp. NITD 19. *Journal of Environmental Engineering* **147** (1), 04020143.

Shi, J. X., Han, H. J. & Xu, C. Y. 2019 A novel enhanced anaerobic biodegradation method using biochar and Fe (OH)3 @biochar for the removal of nitrogen heterocyclic compounds from coal gasification wastewater. *Science of the Total Environment* **697**, 9.

Shukla, O. P. & Kaul, S. M. 1974 Constitutive pyridine degrading system in *Corynebacterium* sp. *Indian Journal of Biochemistry & Biophysics* **11** (3), 201–207.

Singh, S. & Lo, S.-L. 2017 Catalytic performance of hierarchical metal oxides for per-oxidative degradation of pyridine in aqueous solution. *Chemical Engineering Journal* **309**, 753–765.

Singleton, D. R., Ramirez, L. G. & Aitken, M. D. 2009 Characterization of a polycyclic aromatic hydrocarbon degradation gene cluster in a phenanthrene-degrading *Acidovorax* strain. *Applied and Environmental Microbiology* **75** (9), 2613–2620.

Wang, J., Jiang, X., Liu, X., Sun, X., Han, W., Li, J., Wang, L. & Shen, J. 2018 Microbial degradation mechanism of pyridine by *Paracoccus* sp. NJUST30 newly isolated from aerobic granules. *Chemical Engineering Journal* **344**, 86–94.

Watson, G. K. & Cain, R. B. 1975 Microbial metabolism of pyridine ring -metabolic pathways of pyridine biodegradation by soil bacteria. *Biochemical Journal* **146** (1), 157–172.

Zhang, Y., Chang, L., Yan, N., Tang, Y., Liu, R. & Rittmann, B. E. 2014 UV photolysis for accelerating pyridine biodegradation. *Environmental Science & Technology* **48** (1), 649–655.

Zhao, Q. & Liu, Y. 2016 State of the art of biological processes for coal gasification wastewater treatment (vol 34, pg 1064, 2016). *Biotechnology Advances* **34** (8), 1442.

First received 24 November 2023; accepted in revised form 21 March 2024. Available online 2 April 2024